J. Math. Biol. (2016) 73:751–784
DOI 10.1007/s00285-016-0971-y

Mathematical Biology

An avian-only Filippov model incorporating culling of both susceptible and infected birds in combating avian influenza

Nyuk Sian Chong[1,2] · **Benoit Dionne**[1] · **Robert Smith?**[1,3]

Received: 7 June 2015 / Revised: 5 November 2015 / Published online: 10 February 2016

Abstract Depopulation of birds has always been an effective method not only to control the transmission of avian influenza in bird populations but also to eliminate influenza viruses. We introduce a Filippov avian-only model with culling of susceptible and/or infected birds. For each susceptible threshold level S_b, we derive the phase portrait for the dynamical system as we vary the infected threshold level I_b, focusing on the existence of endemic states; the endemic states are represented by real equilibria, pseudoequilibria and pseudo-attractors. We show generically that all solutions of this model will approach one of the endemic states. Our results suggest that the spread of avian influenza in bird populations is tolerable if the trajectories converge to the equilibrium point that lies in the region below the threshold level I_b or if they converge to one of the pseudoequilibria or a pseudo-attractor on the surface of discontinuity. However, we have to cull birds whenever the solution of this model converges to an equilibrium point that lies in the region above the threshold level I_b in order to control the outbreak. Hence a good threshold policy is required to combat bird flu successfully and to prevent overkilling birds.

✉ Robert Smith?
rsmith43@uottawa.ca

Nyuk Sian Chong
nchon077@uottawa.ca

Benoit Dionne
bdionne@uottawa.ca

[1] Department of Mathematics and Statistics, University of Ottawa, 585 King Edward Ave, Ottawa, ON K1N 6N5, Canada

[2] School of Informatics and Applied Mathematics, Universiti Malaysia Terengganu, 21030 Kuala Terengganu, Malaysia

[3] Faculty of Medicine, University of Ottawa, 451 Smyth Rd, Ottawa, ON K1H 8M5, Canada

Keywords Dynamical systems · Avian influenza · Filippov model · Culling · Threshold policy

Mathematics Subject Classification 34C05 · 92D30

1 Introduction

Avian influenza is induced by type A viruses. These viruses can be classified into two categories: low pathogenic avian influenza (LPAI) and highly pathogenic avian influenza (HPAI) (Public Health Agency of Canada 2006; Canadian Food Inspection Agency 2012; Centers for Disease Control and Prevention 2012). Infection by LPAI viruses usually causes mild or no illness at all, whereas infection by HPAI viruses can cause severe disease with high disease-death rate. These two types of viruses can potentially infect domesticated birds (such as chickens, quails and turkeys) rapidly, as well as wild birds and humans (Public Health Agency of Canada 2006; Canadian Food Inspection Agency 2012; Centers for Disease Control and Prevention 2012).

Waterfowl are carriers of the avian influenza viruses but do not show any symptoms. They spread the virus through excretions; the virus can be easily spread to domesticated birds when they come in contact with waterfowl or via contaminated area/objects. As a result, this allows the virus to proliferate, which may further induce viral mutation (Public Health Agency of Canada 2006; Centers for Disease Control and Prevention 2012; Jacob et al. 2013).

Currently, there is no effective treatment for birds infected with avian influenza. Although vaccination, biosecurity and surveillance measures reduce the infection rate, these measures do not eliminate the virus (Canadian Food Inspection Agency 2012; International Animal Health Organisation 2015; Jacob et al. 2013). Thus, whenever a highly pathogenic avian influenza outbreak occurs, culling birds is usually an effective method to control the spread of the disease. However, susceptible birds are also at risk of being killed in the course of preventing the disease (FAO 2006, 2008, 2011; Centers for Disease Control and Prevention 2012; International Animal Health Organisation 2015; Kimman et al. 2013; Perez and Garcia-Sastre 2013). Hence an efficient culling strategy is needed to avoid overkilling and reduce the economic impact, particularly where the poultry business is concerned (FAO 2008, 2011; Centers for Disease Control and Prevention 2012; Gulbudak and Martcheva 2013).

A number of studies involving the culling strategy in bird populations to combat avian influenza have been carried out (Dorigatti et al. 2010; Gulbudak and Martcheva 2013; Iwami et al. 2008, 2009; Menach et al. 2006; Shim and Galvani 2009). Menach et al. (2006) proposed a model that employs stochastic and deterministic processes to examine the impact and efficiency of control strategies. For instance, the spread of the disease within a farm is modelled stochastically by discrete-time model formulation, whereas the changes of farm's disease status is studied by using a deterministic model. Based on the results obtained, an immediate culling of infected flocks upon an accurate and quick diagnosis will be better at controlling the outbreak compared to the strategy of only stamping out the surrounding flocks.

Shim and Galvani (2009) proposed a mathematical model parameterized by clinical, epidemiological and poultry data to assess the evolutionary consequences of mass avian depopulation on both host and pathogen. They also investigated the selection of a dominant allele that confers resistance against avian influenza and the level of pathogenicity of influenza. Their results showed that, by increasing the culling rate, less host resistance is needed to eradicate the disease and the selection for the resistant allele would be reduced. As a consequence, the implementation of mass depopulation would elevate the virulence level of influenza. So, although an avian influenza outbreak can be eliminated by employing mass avian culling control strategy, it brings several detrimental evolutionary consequences such as the decreasing of influenza resistance and the increasing of host mortality and influenza virulence.

Dorigatti et al. (2010) considered an SEIR (Susceptible-Exposed-Infected-Removed) model with a spatial transmission kernel to model the diffusion of H7N1 in Italy. The infection of H7N1 between farms was investigated. They found that the transmissibility of virus between the first phase and the subsequent phases is decreasing, and there is a variation of susceptibility in between poultry species. Further, they discovered that banning restocking on empty farms was the most effective control method.

During the emerging phase of an infectious disease, applying control measures to prevent the infection may be disregarded by the public. However, when the number of infected individuals has gone beyond a certain threshold level, the public will be alerted and immediate actions have to be taken in order to avoid a deadly outbreak. Hence a good threshold policy is required to provide useful information in disease-management strategy not only to the public but also to the public authorities, so that the disease can be eradicated or at least reduced to a minimum level (Tang et al. 2012; Xiao et al. 2012; Zhao et al. 2013).

Xiao et al. (2013) proposed an infectious disease model with a piecewise smooth incidence rate that incorporated media/psychology effects by converting the implicitly defined classical model based on the properties of the Lambert W function. The global dynamics of this system were analyzed. They discovered that the disease-free equilibrium is globally asymptotically stable if the basic reproduction number is less than one, whereas the endemic equilibrium is globally stable whenever the basic reproduction number is larger than one. Moreover, the effect of media does not affect the epidemic threshold or disease eradication. However, it does reduce the number of infected individuals and the prevalence significantly.

Furthermore, Wang and Xiao (2014) designed a Filippov SIR (Susceptible-Infected-Recovered) model to describe the media effects on the spread of infectious diseases. The mass media will have an effect whenever the number of infected individuals reaches a certain threshold level. A bifurcation analysis was conducted and all possible dynamic behaviours were determined. Based on the primary results, the model will achieve stability either at the two endemic equilibria or the pseudoequilibrium. They inferred that a good threshold policy with media coverage can assist in controlling and combating an emerging infectious disease.

In Sect. 2 of this paper, we propose a Filippov avian-only model incorporating culling of susceptible and/or infected birds. We extend our previous work on the avian-only model (Chong and Smith? 2015) by considering not only culling of infected birds but also the effort to stamp out susceptible birds if the numbers of susceptible and infected birds exceed certain threshold levels. Previously, we only considered culling of infected birds for the avian-only model as a control measure (Chong and Smith? 2015). In Sects. 3–6, we analyse all the possible dynamics of this model by varying the threshold levels of the infected and susceptible birds. We prove the existence of equilibria, *pseudoequilibria* and *pseudo-attractors*. The prefix *pseudo* was added to equilibria and attractors to distinguish them from the standard equilibria and attractors. For a pseudoequilibrium, some orbits may converge to it in a finite time. For the pseudo-attractor, all orbits will converge to it in a finite time. Finally, Sect. 7 will present several concluding remarks together with the discussion pertaining to the study.

2 The avian-only Filippov model

In this section, we propose a threshold policy in an avian-only model with culling of susceptible and/or infected birds. We only consider domestic birds for the avian population. To control the spread of the disease and reduce the transmission level, immediate action (i.e., a culling strategy) has to be taken once the numbers of susceptible and infected birds exceed the threshold levels.

In this paper, we will focus on the effects of tolerance thresholds of susceptible birds S_b and infected birds I_b, which can provide useful information for disease management. Namely, in which cases do we have to apply culling of susceptible and/or infected birds in order to suppress the infection rate? We use a Filippov model to determine threshold criteria for culling. Filippov models consist of ordinary differential equations with discontinuous conditions on the derivatives, whereby the solution undergoes a rapid change in motion when certain conditions are met.

We assume that the infection is within the tolerable range when the number of infected birds I is less than the tolerance threshold I_b, so no control strategy is required under this condition, and that an outbreak might occur if $I > I_b$, which requires a control strategy to reduce the infection to a safer level. In this model, we do not apply any control strategies when $I < I_b$. However, for $I > I_b$, we kill only infected birds at a rate of c_2 if the number of susceptible birds S is less than the threshold level S_b, and we cull both susceptible and infected birds at rates of c_1 and c_3 respectively if $S > S_b$. We assume that $c_2 < c_3$ and $c_1, c_2, c_3 > 0$ in this model. We not only consider culling infected birds with a higher cull rate c_3 when $S > S_b$ but we also reduce the population of susceptible birds. The reason for this choice is that we may have a lot of susceptible birds that may get infected by avian influenza later and more severely affect the outbreak.

We consider an avian-only population that is divided into susceptible and infected birds. Infected birds are assumed to remain in the infected class in this model. The sum of $S(t)$ and $I(t)$ is the total population of domestic birds $N(t)$ at time t. This avian-only Filippov model is governed by nonlinear ordinary differential equations with discontinuous right-hand sides as follows:

$$\begin{pmatrix} S' \\ I' \end{pmatrix} = F(S, I) \equiv \begin{pmatrix} \Lambda - \beta SI - (\mu + u_1)S \\ \beta SI - (\mu + d + u_2)I \end{pmatrix} \tag{2.1}$$

with

$$(u_1, u_2) = \begin{cases} (0, 0) & \text{for } I < I_b \\ (0, c_2) & \text{for } S < S_b \text{ and } I > I_b \\ (c_1, c_3) & \text{for } S > S_b \text{ and } I > I_b, \end{cases} \tag{2.2}$$

where $S_b, I_b > 0$ are the tolerance thresholds, Λ (individual/day) is the bird inflow, β (/day $\times$ /individual) is the rate at which birds contract avian influenza, μ (/day) is the natural death rate of birds, and d (/day) is the additional disease-specific death rate due to avian influenza in birds.

We divide the S, I space $\mathbb{R}^2_+$ into five regions as follows:

$$G_1 \equiv \left\{(S, I) \in \mathbb{R}^2_+ : I < I_b\right\}$$
$$G_2 \equiv \left\{(S, I) \in \mathbb{R}^2_+ : S < S_b \text{ and } I > I_b\right\}$$
$$G_3 \equiv \left\{(S, I) \in \mathbb{R}^2_+ : S > S_b \text{ and } I > I_b\right\}$$
$$M_1 \equiv \left\{(S, I) \in \mathbb{R}^2_+ : I = I_b\right\}$$

and

$$M_2 \equiv \{(S, I) \in \mathbb{R}^2_+ : S = S_b \text{ and } I > I_b\}.$$

The dynamics in region G_i are governed by f_i, for $i = 1, 2$ and 3, where

$$f_1(S, I) = \begin{pmatrix} \Lambda - \beta SI - \mu S \\ I\big(\beta S - (\mu + d)\big) \end{pmatrix} \tag{2.3}$$

$$f_2(S, I) = \begin{pmatrix} \Lambda - \beta SI - \mu S \\ I\big(\beta S - (\mu + d + c_2)\big) \end{pmatrix} \tag{2.4}$$

and

$$f_3(S, I) = \begin{pmatrix} \Lambda - \beta SI - (\mu + c_1)S \\ I\big(\beta S - (\mu + d + c_3)\big) \end{pmatrix}. \tag{2.5}$$

Moreover, the normal vectors that are perpendicular to M_1 and M_2 are defined as $n_1 = (0, 1)^T$ and $n_2 = (1, 0)^T$, respectively.

To give a sense of the flow of the dynamical system on the boundaries M_i between the regions G_i, we use Filippov's convex method (Filippov 1988). The basic idea of Filippov's method is to replace the vector field F in (2.1) by the set-valued function $\hat{F}$, where $\hat{F}(S, I)$ is the closed convex hull of the set

$$\left\{\begin{pmatrix} U \\ V \end{pmatrix} : \begin{pmatrix} U \\ V \end{pmatrix} = \lim_{(u,v)\to(S,I)} F(u, v) \text{ for } (u, v) \in G_i\right\}.$$

Then (2.1) becomes

$$\begin{pmatrix} S' \\ I' \end{pmatrix} \in \hat{F}(S, I).$$

There is a theory of existence and uniqueness of solutions for such systems. Since $F|_{G_i}$ is continuously differentiable on the closure of G_i, we may give a simple interpretation of Filippov's method. At the points (S, I) where F is continuous, $\hat{F}(S, I) = \{F(S, I)\}$, and hence we may still use the formulation in (2.1). To be able to write

$$\begin{pmatrix} S' \\ I' \end{pmatrix} = F(S, I).$$

at the points $(S, I) \in M_i$ ($i = 1$ or 2) where F is discontinuous, we choose a representative value for $\hat{F}(S, I)$ as follows. Let $F_+(S, I) = \lim_{(u,v)\to(S,I)} F(u, v)$ for (u, v) on one side of M_i and $F_-(S, I) = \lim_{(u,v)\to(S,I)} F(u, v)$ for (u, v) on the other side of M_i. Then

$$\hat{F}(S, I) = \{\alpha F_+(S, I) + (1 - \alpha)F_-(S, I) : 0 \leq \alpha \leq 1\}.$$

At a point (S, I) of M_i where the flow of F approaches (S, I) on one side of M_i and moves away from (S, I) on the other side of M_i, we may choose any vector in $\hat{F}(S, I)$. This will not influence the dynamics because this vector will point in the local direction of the vector field.

The more interesting situation is when the flow of F approaches M_i from all sides or moves away from M_i from all sides.

Definition 2.1 The set of all points (S, I) on M_i such that the flow of F (outside M_i) approaches (S, I) from all sides is an attraction sliding mode. When the attraction sliding mode is formed of only one point, we call this point a pseudo-attractor. The repulsion sliding mode is the set of all points (S, I) on M_i such that the flow of F (outside M_i) moves away from (S, I).

At a point (S, I) on M_i where the flow of F approaches (S, I) from both sides (or moves away from both sides), we choose $F(S, I) = \alpha F_+(S, I) + (1 - \alpha)F_-(S, I)$, where $\alpha = (n_i^\top F_-(S, I))/(n_i^\top (F_-(S, I) - F_+(S, I)))$ and n_i is a normal vector to M_i. With this choice, the flow entering the sliding mode will remain on it for at least a finite time. We have $n_1 = (0, 1)^T$ and $n_2 = (1, 0)^T$.

The vector field F that we defined on sliding modes may have an equilibrium point; such an equilibrium point is called a *pseudoequilibrium*. The major difference between this type of equilibrium point and the classical equilibrium points for a continuously differentiable vector field in $\mathbb{R}^2$ is that some of the orbits inside G_i may converge to this equilibrium in a finite period as time increases or decreases.

We now identify the existence of a positively invariant and globally (in $\mathbf{R}_+^2$) attracting region for the system (2.1).

Lemma 2.2 *$D \equiv \{(S, I) \in \mathbb{R}_+^2 : S + I \leq \frac{\Lambda}{\mu}\}$ is a positively invariant and attracting region in $\mathbf{R}_+^2$ for the system* (2.1).

If you ignore the lines M_1 and M_2, where the vector field F is discontinuous, the proof will look like this. Let $N = S + I$. Taking the sum of S' and I' given by (2.1) yields

$$N' = \Lambda - \mu(S + I) - u_1 S - (d + u_2)I \leq \Lambda - \mu N.$$

Thus

$$\frac{d}{ds}\big(N(s)e^{\mu s}\big) = e^{\mu s}(N'(s) + \mu N(s)) \leq \Lambda e^{\mu s}.$$

Integrating both sides between 0 and t gives

$$N(t)e^{\mu t} - N(0) = \int_0^t \frac{d}{ds}\big(N(s)e^{\mu s}\big)ds \leq \int_0^t \Lambda e^{\mu s} ds = \frac{\Lambda}{\mu}\left(e^{\mu t} - 1\right).$$

If $N(0) \leq \frac{\Lambda}{\mu}$, then we get

$$N(t)e^{\mu t} \leq N(0) + \frac{\Lambda}{\mu}\left(e^{\mu t} - 1\right) \leq \frac{\Lambda}{\mu}e^{\mu t},$$

and thus $N(t) \leq \frac{\Lambda}{\mu}$. This proves that D is positively invariant.

To prove that D is attractive, let's suppose that $N > \frac{\Lambda}{\mu}$ and let $\phi = \frac{\Lambda}{\mu}$. We have proved above that $N' \leq \Lambda - \mu N$. Thus $N' \leq \mu\phi - \mu N = \mu(\phi - N) < 0$.

A simple but lengthy justification could be given to handle the situation where the vector field F is discontinuous.

We have from the lemma that the ω-limit sets of (2.1) are contained in D.

2.1 The system f_1

In this section, we study the dynamics of f_1 given by (2.3) on $\mathbb{R}^2_+$. In particular, we examine the linear stability of the two equilibria of this system: the disease-free equilibrium (DFE) $E_{10} = \left(\frac{\Lambda}{\mu}, 0\right)$ and the endemic equilibrium (EE)

$$E_{11} \equiv (h_1, g_1) = \left(\frac{\mu + d}{\beta}, \frac{\Lambda\beta - \mu(\mu + d)}{\beta(\mu + d)}\right).$$

The basic reproduction number (Driessche and Watmough 2002; Li et al. 2011) of this system is

$$R_1 = \frac{\Lambda\beta}{\mu(\mu+d)}.$$

The Jacobian matrix for (2.3) is

$$J_1(S,I) = \begin{pmatrix} -\beta I - \mu & -\beta S \\ \beta I & \beta S - (\mu+d) \end{pmatrix}.$$

Theorem 2.3 *E_{10} is locally asymptotically stable for $R_1 < 1$ and unstable for $R_1 > 1$.*

Proof The eigenvalues of $J_1(E_{10})$ are obtained from

$$|J_1(E_{10}) - \lambda I| = -(\mu+\lambda)\left(\frac{\Lambda\beta - \mu(\mu+d)}{\mu} - \lambda\right) = 0.$$

Thus $\lambda = -\mu < 0$ and $\lambda = \frac{\Lambda\beta-\mu(\mu+d)}{\mu}$ is negative for $R_1 < 1$ and positive for $R_1 > 1$, where all parameters are positive. □

Theorem 2.4 *E_{11} is locally asymptotically stable for $R_1 > 1$.*

Proof The eigenvalues of $J_1(E_{11})$ are

$$\lambda_\pm = \frac{1}{2}\left(-\frac{\Lambda\beta}{\mu+d} \pm \sqrt{\nu}\right), \quad \text{where} \quad \nu = \left(\frac{\Lambda\beta}{\mu+d}\right)^2 - 4\left(\Lambda\beta - \mu(\mu+d)\right).$$

For $R_1 > 1$, we have $\Lambda\beta - \mu(\mu+d) > 0$. Hence $\nu < \left(\frac{\Lambda\beta}{\mu+d}\right)^2$ and $\lambda_\pm < 0$. □

2.2 The system f_2

This time, we study the dynamics of f_2 given by (2.4) on $\mathbb{R}^2_+$. There are two equilibria for this system: the EE,

$$E_{21} \equiv (h_2, g_2) = \left(\frac{\mu+d+c_2}{\beta}, \frac{\Lambda\beta - \mu(\mu+d+c_2)}{\beta(\mu+d+c_2)}\right),$$

and the DFE, $E_{20} = \left(\frac{\Lambda}{\mu}, 0\right)$. To determine their linear stability, we need the basic reproduction number

$$R_2 = \frac{\Lambda\beta}{\mu(\mu+d+c_2)}$$

of this model. The Jacobian matrix of (2.4) is

$$J_2(S,I) = \begin{pmatrix} -\beta I - \mu & -\beta S \\ \beta I & \beta S - (\mu+d+c_2) \end{pmatrix}.$$

Theorem 2.5 *The DFE E_{20} is locally asymptotically stable if $R_2 < 1$ and unstable if $R_2 > 1$.*

The proof of this theorem is similar to the proof of Theorem 2.3.

Theorem 2.6 *The EE E_{21} is locally asymptotically stable if $R_2 > 1$.*

Proceeding as in the proof of Theorem 2.4, one can show that E_{21} is either a stable spiral or a stable node if $R_2 > 1$.

2.3 The system f_3

Finally, we study the dynamics of f_3 given by (2.5) on $\mathbb{R}^2_+$. There are two equilibria for this system, the DFE, $E_{30} = (\frac{\Lambda}{\mu+c_1}, 0)$, and the EE, $E_{31} \equiv (h_3, g_3) = (\frac{\mu+d+c_3}{\beta}, \frac{\Lambda\beta-(\mu+c_1)(\mu+d+c_3)}{\beta(\mu+d+c_3)})$. The basic reproduction number of (2.5) is $R_3 = \frac{\Lambda\beta}{(\mu+c_1)(\mu+d+c_3)}$.

Theorem 2.7 *The DFE E_{30} is locally asymptotically stable if $R_3 < 1$ and unstable whenever $R_3 > 1$.*

Theorem 2.7 is proved as Theorem 2.3 is proved.

Theorem 2.8 *The EE E_{31} is locally asymptotically stable if $R_3 > 1$.*

A proof similar to the proof of Theorem 2.4 shows that all eigenvalues of the linearization of (2.5) at E_{31} are either negative real numbers or complex numbers with negative real parts.

3 Case A: $S_b < h_1$

In this and the following three sections, we determine the existence of sliding modes on M_1 and M_2 and study the dynamics of (2.1) and (2.2). We have $h_1 < h_2 < h_3$ and $g_3 < g_2 < g_1$. We consider the 16 cases generated by $S_b < h_1$, $h_1 < S_b < h_2$, $h_2 < S_b < h_3$ and $h_3 < S_b$, and $I_b < g_3$, $g_3 < I_b < g_2$, $g_2 < I_b < g_1$ and $g_1 < I_b$. They each require a distinct mathematical analysis. However, we will show in the conclusion that many of these cases are identical from a biological point of view. The endemic equilibrium may mathematically change from one case to the other but may still produce the same biological phenomena.

The conclusions of the results in Sects. 3–6 are summarized in the table at the end of the paper. We list the equilibria of the dynamical system (2.1) when the thresholds S_b and I_b vary, as well as the corresponding culling strategy to be implemented.

3.1 Existence of a sliding mode on M_1 and its dynamics

There are several types of regions on a discontinuity surface and several types of equilibrium points for a Filippov system. See Appendices A and B of Chong and Smith? (2015), respectively.

Proposition 3.1 (Zhao et al. 2013) *If* $\langle n_1, f_1\rangle > 0$ *and* $\langle n_1, f_3\rangle < 0$ *on* $\Omega_1 \subset M_1$, *then* Ω_1 *is a sliding region.*

From $\langle n_1, f_1\rangle > 0$ and $\langle n_1, f_3\rangle < 0$, we get

$$h_1 = \frac{\mu + d}{\beta} < S < \frac{\mu + d + c_3}{\beta} = h_3.$$

Thus

$$\Omega_1 = \{(S, I) \in M_1 : S_b < h_1 < S < h_3\}. \tag{3.1}$$

Sliding-mode equations can be found by using Filippov convex method (Filippov 1988; Leine 2000) as follows:

$$\begin{pmatrix} S' \\ I' \end{pmatrix} = \psi f_1 + (1-\psi) f_3 \quad \text{, where } \psi = \frac{\langle n_1, f_3\rangle}{\langle n_1, f_3 - f_1\rangle}.$$

Thus

$$\begin{pmatrix} S' \\ I' \end{pmatrix} = \begin{pmatrix} \Lambda - \beta S I - (\mu + c_1) S + \dfrac{c_1 S\left((\mu + d + c_3) - \beta S\right)}{c_3} \\ 0 \end{pmatrix}. \tag{3.2}$$

The differential equation for S has two steady states, given by

$$S = \frac{B \pm \sqrt{B^2 - 4AC}}{2\beta c_1}, \quad \text{where } A = -\beta c_1, B = c_1(\mu + d) - c_3(\beta I_b + \mu)$$
$$\text{and } C = \Lambda c_3.$$

However, $B^2 - 4AC > B^2 > 0$ because $A < 0$ and $C > 0$. Thus there is only one positive steady state, given by

$$S = h_4 \equiv \frac{B + \sqrt{B^2 - 4AC}}{2\beta c_1}.$$

Hence $E_{S1} = (h_4, I_b) \in \Omega_1 \subset M_1$ is an equilibrium for (3.2) if $h_1 < h_4 < h_3$. It is locally asymptotically stable because

$$\frac{\partial}{\partial S}\left(\frac{-\beta c_1 S^2 + (c_1(\mu + d) - c_3(\beta I_b + \mu))\, S + \Lambda c_3}{c_3}\right)\Bigg|_{E_{S1}} = \frac{-\sqrt{B^2 - 4AC}}{c_3} < 0.$$

We now show that E_{S1} is globally asymptotically stable if

$$g_3 < I_b < g_1. \tag{3.3}$$

We note that the equilibria E_{11}, E_{21} and E_{31} for f_1, f_2 and f_3, respectively, do not appear in this case, because they are outside the considered domain for f_1, f_2 and f_3. For this reason, we call them *virtual equilibria* for (2.1).

Theorem 3.2 *$E_{S1} \in \Omega_1 \subset M_1$ is globally asymptotically stable if $g_3 < I_b < g_1$ and $R_1 > 1$.*

Proof We first prove that there cannot be any periodic solution entirely included in one of the regions G_i. Consider a Dulac function $B_1(S, I) = \frac{1}{SI}$ for $(S, I) \in \mathbb{R}^2_+$. Then

$$\frac{\partial(B_1 f_{1,1})}{\partial S} + \frac{\partial(B_1 f_{1,2})}{\partial I} = \frac{\partial}{\partial S}\left(\frac{\Lambda}{SI} - \beta - \frac{\mu}{I}\right) + \frac{\partial}{\partial I}\left(\beta - \frac{\mu + d}{S}\right) = -\frac{\Lambda}{S^2 I} < 0$$

on $\mathbb{R}^2_+$, where $f_{1,1}$ is the first component of f_1 and $f_{1,2}$ is the second component of f_1. We have a similar result for f_2 and f_3. From Dulac's Theorem (Perko 2001), we know that there will not be any periodic solution included in $\mathbb{R}^2_+ \backslash \{M_1, M_2\}$.

Because the vector field F in (2.1) is discontinuous, we cannot use Dulac's Theorem to prove that there are no periodic solution crossing the regions M_i. However, proceeding as in the proof of Dulac's Theorem, using Green's Theorem, we can reach this conclusion for our system as we now show.

Suppose that Γ is a periodic orbit around Ω_1 as in Fig. 1. Let $\Gamma = \Gamma_1 + \Gamma_2 + \Gamma_3$, where $\Gamma_i = \Gamma \cap G_i$. Let H be the bounded region delimited by Γ and $H_i = H \cap G_i$ for $i = 1, 2$ and 3. Then

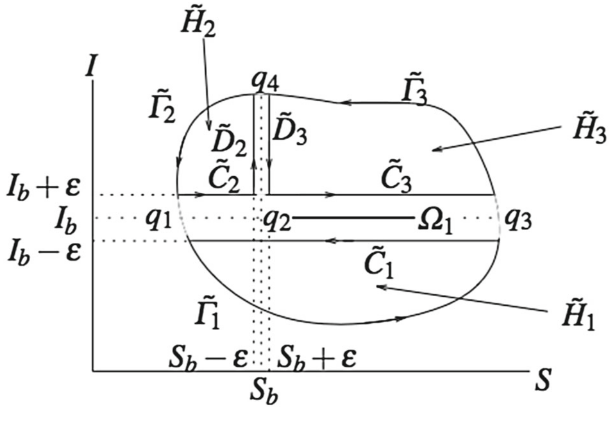

Fig. 1 Limit cycle Γ

$$\iint_H \left(\frac{\partial(B_1F_1)}{\partial S}+\frac{\partial(B_1F_2)}{\partial I}\right)dSdI$$
$$=\sum_{i=1}^{3}\iint_{H_i}\left(\frac{\partial(B_1f_{i,1})}{\partial S}+\frac{\partial(B_1f_{i,2})}{\partial I}\right)dSdI<0, \quad (3.4)$$

where F_1 is the first component of F and F_2 is the second component of F. We have

$$\iint_{H_i}\left(\frac{\partial(B_1f_{i,1})}{\partial S}+\frac{\partial(B_1f_{i,2})}{\partial I}\right)dSdI=\lim_{\epsilon\to 0}\iint_{\tilde{H}_i}\left(\frac{\partial(B_1f_{i,1})}{\partial S}+\frac{\partial(B_1f_{i,2})}{\partial I}\right)dSdI,$$

where $\tilde{H}_i$ is the region bounded by the curves $\tilde{\Gamma}_i$, $\tilde{C}_i$ and $\tilde{D}_i$ (if necessary) as illustrated in Fig. 1. $\tilde{H}_i$ and $\tilde{\Gamma}_i$ depend on ϵ and converge to H_i and Γ_i as ϵ approaches 0.

By applying Green's Theorem to the region $\tilde{H}_1$, we get

$$\begin{aligned}\iint_{\tilde{H}_1}\left(\frac{\partial(B_1f_{1,1})}{\partial S}+\frac{\partial(B_1f_{1,2})}{\partial I}\right)dSdI&=\oint_{\partial\tilde{H}_1}B_1f_{1,1}dI-B_1f_{1,2}dS\\&=\int_{\tilde{\Gamma}_1}B_1f_{1,1}dI-B_1f_{1,2}dS+\int_{\tilde{C}_1}B_1f_{1,1}dI-B_1f_{1,2}dS\\&=-\int_{\tilde{C}_1}B_1f_{1,2}dS\end{aligned} \quad (3.5)$$

because $dS=f_{1,1}dt$ and $dI=f_{1,2}dt$ along $\tilde{\Gamma}_1$, and $dI=0$ along $\tilde{C}_1$. Note that $\partial\tilde{H}_1$ denotes the boundary of $\tilde{H}_1$.

Proceeding as we just did, we get

$$\iint_{\tilde{H}_2}\left(\frac{\partial(B_1f_{2,1})}{\partial S}+\frac{\partial(B_1f_{2,2})}{\partial I}\right)dSdI=\int_{\tilde{D}_2}B_1f_{2,1}dI-\int_{\tilde{C}_2}B_1f_{2,2}dS \quad (3.6)$$

and

$$\iint_{\tilde{H}_3}\left(\frac{\partial(B_1f_{3,1})}{\partial S}+\frac{\partial(B_1f_{3,2})}{\partial I}\right)dSdI=\int_{\tilde{D}_3}B_1f_{3,1}dI-\int_{\tilde{C}_3}B_1f_{3,2}dS. \quad (3.7)$$

From (3.4) to (3.7), we see that

$$\begin{aligned}0&>\sum_{i=1}^{3}\iint_{H_i}\left(\frac{\partial(B_1f_{i,1})}{\partial S}+\frac{\partial(B_1f_{i,2})}{\partial I}\right)dSdI\\&=\lim_{\epsilon\to 0}\left(-\int_{\tilde{C}_1}B_1f_{1,2}dS+\int_{\tilde{D}_2}B_1f_{2,1}dI-\int_{\tilde{C}_2}B_1f_{2,2}dS+\int_{\tilde{D}_3}B_1f_{3,1}dI-\int_{\tilde{C}_3}B_1f_{3,2}dS\right).\end{aligned}$$

If q_1 and q_3 are the intersections of Γ with the line $I = I_b$, q_4 is the intersection of Γ with the line $S = S_b$ with $I > I_b$ and $q_2 = (S_b, I_b)$, then the previous inequality can be written

$$\begin{aligned} 0 > &-\int_{q_{3,1}}^{q_{1,1}} \left(\beta - \frac{\mu + d}{S}\right) dS + \int_{q_{2,2}}^{q_{4,2}} \left(\frac{\Lambda}{SI} - \beta - \frac{\mu}{I}\right) dI - \int_{q_{1,1}}^{q_{2,1}} \left(\beta - \frac{\mu + d + c_2}{S}\right) dS \\ &+ \int_{q_{4,2}}^{q_{2,2}} \left(\frac{\Lambda}{SI} - \beta - \frac{\mu + c_1}{I}\right) dI - \int_{q_{2,1}}^{q_{3,1}} \left(\beta - \frac{\mu + d + c_3}{S}\right) dS \\ &= c_1(\ln q_{4,2} - \ln I_b) + c_2(\ln S_b - \ln q_{1,1}) + c_3(\ln q_{3,1} - \ln S_b) > 0 \end{aligned}$$

since $q_{1,1} < S_b < q_{3,1}$ and $q_{4,2} > I_b$. This is a contradiction. So the periodic solution Γ cannot exist.

Similar computations show that no periodic orbit can cross only M_1 or only M_2.

The condition $R_1 > 1$ implies that E_{10} is unstable. This condition is always satisfied in the model that we consider. □

Remark It should be noted that Dulac's Theorem relies on continuity and hence cannot be applied directly to Filippov systems. However, our proof follows the same idea as Dulac's Theorem, by using Green's Theorem and considering the boundary to be away from the discontinuities, in order to produce the result.

3.2 Sliding mode on M_2 and its dynamics

Proposition 3.3 (Zhao et al. 2013) *The sliding region Ω_2 is the set of all points on M_2 such that $\langle n_2, f_2\rangle > 0$ and $\langle n_2, f_3\rangle < 0$.*

We have $\langle n_2, f_2\rangle > 0$ for $I < g_4 \equiv (\Lambda - \mu S_b)/(\beta S_b)$ and $\langle n_2, f_3\rangle < 0$ for $I > g_5 \equiv \big(\Lambda - (\mu + c_1)S_b\big)/(\beta S_b)$. We have $g_5 < g_4$ because $c_1 > 0$. So, as long as $I_b < g_4$, we get the sliding domain $\Omega_2 \subset M_2$ defined as

$$\Omega_2 = \Big\{(S, I) \in M_2 : \max\{g_5, I_b\} < I < g_4\Big\}. \tag{3.8}$$

The condition $S_b < h_1$ implies that $g_3 < g_5$ because $c_3 > 0$, and $g_1 < g_4$. Thus

$$g_3 < g_1, g_5 < g_4. \tag{3.9}$$

There is no sliding domain on M_2 for $I_b > g_4$.

Again, by the Filippov convex method, the sliding mode equation on Ω_2 is given by

$$\begin{pmatrix} S' \\ I' \end{pmatrix} = \psi_2 f_2 + (1 - \psi_2) f_3, \quad \text{where } \psi_2 = \frac{\langle n_2, f_3\rangle}{\langle n_2, f_3 - f_2\rangle}.$$

Thus

$$\begin{pmatrix} S' \\ I' \end{pmatrix} = \begin{pmatrix} 0 \\ I\left(\beta S - (\mu + d + c_3) + \dfrac{(c_3 - c_2)\,(\beta SI + (\mu + c_1)S - \Lambda)}{c_1 S}\right) \end{pmatrix}. \quad (3.10)$$

System (3.10) has an obvious equilibrium point given by $E_{S2} \equiv (S_b, g_6)$, where

$$g_6 = \frac{c_1 S_b\,((\mu + d + c_3) - \beta S_b) + (c_3 - c_2)\,(\Lambda - S_b(\mu + c_1))}{\beta S_b(c_3 - c_2)}.$$

This becomes a pseudoequilibrium in our system only if

$$\max\{g_5, I_b\} < g_6 < g_4. \quad (3.11)$$

However, it is unstable on Ω_2.

Theorem 3.4 *E_{S2} is an unstable sliding equilibrium on $\Omega_2 \subset M_2$. This is true independently of the value of S_b.*

Proof

$$\frac{\partial}{\partial I}\left(\frac{I\,\big(c_1 S_b\big(\beta S_b - (\mu + d + c_3)\big) + (c_3 - c_2)\big(S_b(\mu + c_1) - \Lambda\big) + \beta S_b(c_3 - c_2)I\big)}{c_1 S_b}\right)\Bigg|_{g_6}$$
$$= \frac{c_1 S_b\big((\mu + d + c_3) - \beta S_b\big) + (c_3 - c_2)\big(\Lambda - S_b(\mu + c_1)\big)}{c_1 S_b} > 0$$

because $g_6 > 0$ and $c_3 > c_2$. □

3.3 Stability of the endemic states

In this section, we are going to investigate the stability of endemic states with a fixed tolerance threshold $S_b < h_1$ as we vary the tolerance threshold I_b. Since $S_b < h_1 < h_2$ in Case A, the equilibrium E_{21} is not present in the system (it is a virtual equilibrium) for any values of I_b. So there is no real equilibrium in region G_2. However, equilibria E_{11} and E_{31} may be present depending on the value of the tolerance threshold I_b.

Moreover, we assume that $R_1 > 1$. Thus the equilibrium E_{10} on the S-axis is unstable according to Theorem 2.3.

3.3.1 Case 1: $I_b < g_3 < g_2 < g_1$

In this case, E_{11} and E_{21} are not present in the system (2.1) but E_{31} is. $E_{S1} \notin \Omega_1 \subset M_1$ since (3.3) is not satisfied. Moreover, since $S_b < h_1 = \frac{\mu+d}{\beta}$, we have

$$g_6 = g_4 + \frac{c_1(\mu + d + c_2 - \beta S_b)}{\beta(c_3 - c_2)} > g_4.$$

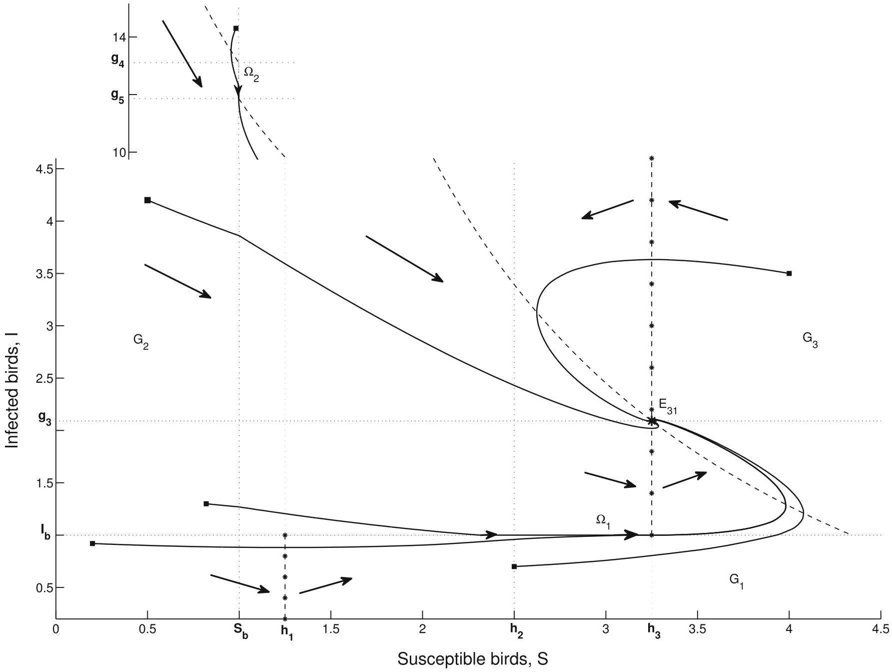

Fig. 2 E_{31} is globally asymptotically stable if $R_1 > 1$, $S_b < h_1$ and $I_b < g_3 < g_2 < g_1$. *Inset* Behaviour when the number of infected birds is large

Thus E_{S2} is not in Ω_2. We claim that E_{31} is globally asymptotically stable if $I_b < g_3 < g_2 < g_1$.

Theorem 3.5 *E_{31} is globally asymptotically stable if $I_b < g_3 < g_2 < g_1$ and $R_1 > 1$.*

Proof The proof is identical to the proof of Theorem 3.2. □

From Fig. 2, where $I_b = 1$ is chosen, we can see that all solutions of model (2.1) will approach E_{31} as $t \to \infty$ as stated in Theorem 3.5. Note that for the chosen parametric values, we have $R_1 > 1$ and E_{10} is unstable.

Throughout this paper, the S-nullclines and I-nullclines of model (2.1) are represented by the dashed curves and asterisk dashed lines, respectively. The curve $\{(S, I) \in \mathbb{R}^2_+ : I = \frac{1}{\beta}(\frac{\Lambda}{S} - \mu)\}$ is the S-nullcline of systems f_1 and f_2, whereas the curve $\{(S, I) \in \mathbb{R}^2_+ : I = \frac{1}{\beta}(\frac{\Lambda}{S} - (\mu + c_1))\}$ is the S-nullcline of system f_3. Furthermore, $S = h_1, h_2$ and h_3 are the I-nullclines of systems f_1, f_2 and f_3, respectively. All associated parameters that are used in the numerical simulations are stated in Table 1. Nevertheless, there is one exception: to get all figures of manageable size, we define $\mu = 0.4$. For Case A, we pick $S_b = 1$.

3.3.2 *Case 2: $g_3 < I_b < g_2 < g_1$ or $g_3 < g_2 < I_b < g_1$*

In both cases, E_{11}, E_{21} and E_{31} are virtual equilibria because $g_1 > I_b$, $h_2 > S_b$ and $g_3 < I_b$ respectively. Thus, E_{11}, E_{21} and E_{31} are not present in system (2.1).

Table 1 Avian-only model (2.1) parameters

	Description	Sample value	Units	References
Λ	Bird inflow	2060/365	Individuals per day	Martcheva (2014)
μ	Natural death of birds	$1/(2 \times 365)$	Per day	Tuncer and Martcheva (2013)
β	Rate at which birds contract avian influenza	0.4	Per individual per day	Gumel (2009)
d	Disease death rate due to avian influenza in birds	0.1	Per day	Tuncer and Martcheva (2013)
c_1	Culling rate of susceptible birds for $S > S_b$ and $I > I_b$	0.5	Per day	Assumed
c_2	Culling rate of infected birds for $S < S_b$ and $I > I_b$	0.5	Per day	Assumed
c_3	Culling rate of infected birds for $S > S_b$ and $I > I_b$	0.8	Per day	Assumed

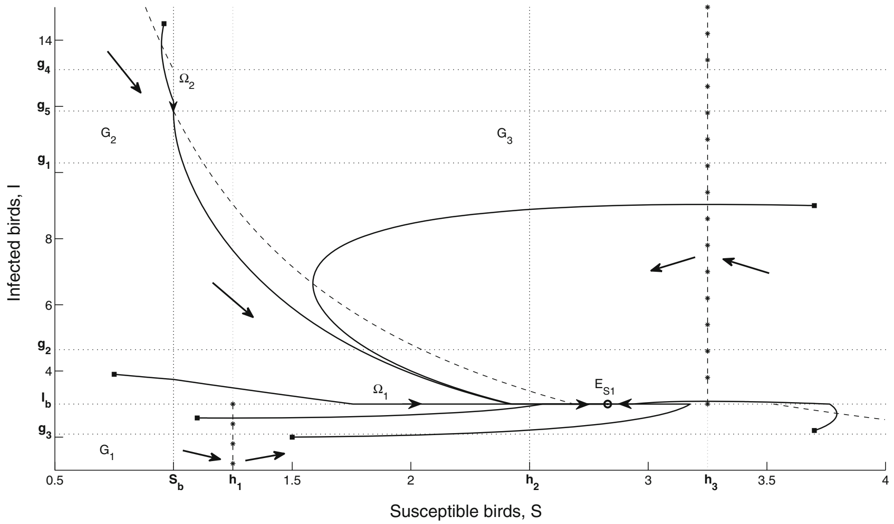

Fig. 3 $E_{S1} \in \Omega_1 \subset M_1$ is globally asymptotically stable if $S_b < h_1$, $g_3 < I_b < g_2 < g_1$ and $R_1 > 1$

$E_{S1} \in \Omega_1 \subset M_1$ is a pseudoequilibrium since (3.3) is satisfied. Moreover, E_{S1} is globally asymptotically stable according to Theorem 3.2.

Theorem 3.6 *E_{S1} is a globally asymptotically stable pseudoequilibrium if $g_3 < I_b < g_2 < g_1$ or $g_3 < g_2 < I_b < g_1$, and $R_1 > 1$.*

The phase portrait for Case 2 with $g_3 < I_b < g_2 < g_1$ is represented in Fig. 3, where $I_b = 3$ is chosen. The phase portrait for $g_3 < g_2 < I_b < g_1$ is similar to Fig. 3 and will not be given.

3.3.3 Case 3: $g_3 < g_2 < g_1 < I_b$

We have the equilibrium $E_{11} \in G_1$ because $g_3 < g_2 < g_1 < I_b$. However, this condition also implies that E_{21} and E_{31} are not present in the system. Moreover, $E_{S1} \notin \Omega_1 \subset M_1$ since (3.3) is not satisfied.

Theorem 3.7 *There is no closed orbit lying in region G_1.*

Proof We have $f_{1,1} = \Lambda - \beta SI - \mu S$ and $f_{1,2} = \beta SI - (\mu + d)I$. Consider a Dulac function $B_1(S, I) = \frac{1}{SI}$ for all $(S, I) \in G_1$. We get

$$
\begin{aligned}
\frac{\partial\big(B_1 f_{1,1}\big)}{\partial S} + \frac{\partial\big(B_1 f_{1,2}\big)}{\partial I} &= \frac{\partial}{\partial S}\Big(\frac{\Lambda}{SI} - \beta - \frac{\mu}{I}\Big) + \frac{\partial}{\partial I}\Big(\beta - \frac{\mu + d}{S}\Big) \\
&= -\frac{\Lambda}{S^2 I} \\
&< 0 \quad \forall (S, I) \in G_1.
\end{aligned}
$$

Therefore, by the Bendixson–Dulac theorem, there is no closed orbit lying entirely within region G_1. □

Theorem 3.8 *E_{11} is globally asymptotically stable if $g_3 < g_2 < g_1 < I_b$ and $R_1 > 1$.*

Proof We define regions D_1, D_2, D_3 and D_4 as follows:

$$
\begin{aligned}
D_1 &= \big\{(S, I) \in \mathbb{R}^2_+ : S \le h_3 \text{ and } I > I_b\big\}, \\
D_2 &= \big\{(S, I) \in \mathbb{R}^2_+ : S > h_3 \text{ and } I > I_b\big\}, \\
D_3 &= \left\{(S, I) \in \mathbb{R}^2_+ : I > \frac{1}{\beta}\left(\frac{\Lambda}{S} - \mu\right) \text{ and } I \le I_b\right\} \text{ and} \\
D_4 &= \left\{(S, I) \in \mathbb{R}^2_+ : I < \frac{1}{\beta}\left(\frac{\Lambda}{S} - \mu\right) \text{ and } I \le I_b\right\}.
\end{aligned}
$$

The vector field in each region is denoted by arrows, as shown in Fig. 4 with $S_b = 1$ and $I_b = 12$. The flow to the right of the S-nullcline is moving to the left, while to the left of the S-nullcline it is moving to the right.

In addition, by Theorems 2.4 and 3.7, E_{11} is locally asymptotically stable and there is no limit cycle in region G_1. The possible trajectories for this case are as follows:

(i) A trajectory with initial point in region D_4 either converges to E_{11} directly or moves downward for $S < h_1$, then upward for $S > h_1$ and finally crosses the S-nullcline to enter the region D_3 and converge to E_{11}.

(ii) A trajectory with initial point in region D_3 converges to E_{11} directly or moves upward for $S > h_1$, then downward for $S < h_1$ and finally crosses the S-nullcline to enter the region D_4 and converge to E_{11}. An orbit starting in D_3 may also go up until it enters the region D_2 through $I = I_b$ or reaches the sliding domain. In both cases, the orbit goes on to enter D_3 or D_4 with $S < h_1$ and converges to E_{11}.

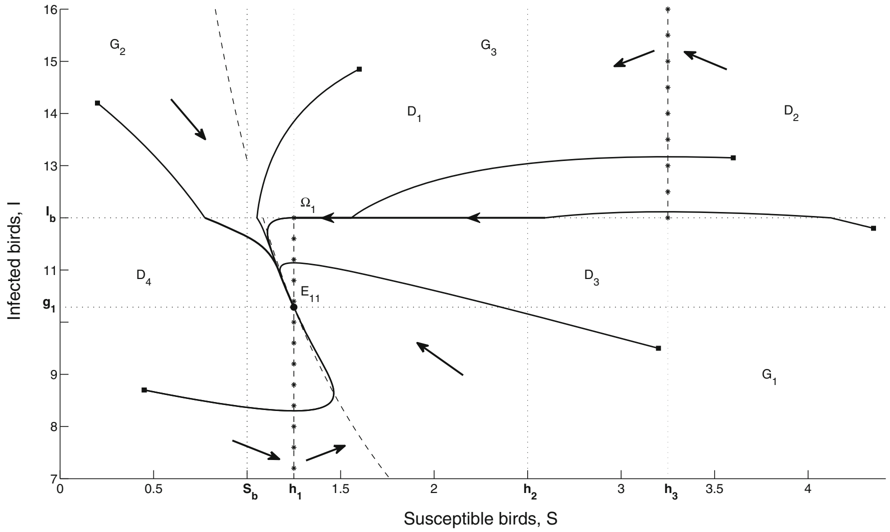

Fig. 4 E_{11} is globally asymptotically stable if $S_b < h_1$, $g_3 < g_2 < g_1 < I_b$ and $R_1 > 1$

(iii) A trajectory that begins in region D_1 moves downward to either enter the region D_3 through $I = I_b$ or the region D_4.

(iv) A trajectory with initial condition in region D_2 moves to the left to either enter the region D_1 through the line $S = h_3$ and then heads to region D_3 or D_4 with $S < h_1$. In all cases, the orbit finally converges to E_{11}.

Since E_{10} is unstable whenever $R_1 > 1$, we conclude that E_{11} is globally asymptotically stable in $\mathbb{R}^2_+$ if $g_3 < g_2 < g_1 < I_b$. □

4 Case B: $h_1 < S_b < h_2$

We will proceed as in Sect. 3 to study the dynamics of (2.1) including the sliding mode on M_1 and M_2 and the stability of endemic states.

4.1 Sliding mode on M_1 and its dynamics

For Case B, we have two sliding domains on M_1.

$$\Omega_3 = \{(S, I) \in M_1; h_1 < S < S_b\}$$

and

$$\Omega_4 = \{(S, I) \in M_1; S_b < S < h_3\}.$$

The dynamics on $\Omega_4 \subset M_1$ are described by (3.2), whereas on $\Omega_3 \subset M_1$, they are governed by

$$\begin{pmatrix} S' \\ I' \end{pmatrix} = \begin{pmatrix} \Lambda - \beta I_b S - \mu S \\ 0 \end{pmatrix}. \tag{4.1}$$

There is a sliding equilibrium for (4.1) at $E_{S3} = (h_5, I_b)$, where $h_5 = \frac{\Lambda}{\beta I_b + \mu}$, and a sliding equilibrium for (3.2) at $E_{S1} = (h_4, I_b)$.

E_{S3} is a pseudoequilibrium if

$$h_1 < h_5 < S_b \tag{4.2}$$

and E_{S1} is a pseudoequilibrium if

$$S_b < h_4 < h_3. \tag{4.3}$$

Proposition 4.1 *We have*

$$h_1 < h_5 < S_b \Leftrightarrow g_4 < I_b < g_1 \tag{4.4}$$

and

$$S_b < h_4 < h_3 \Leftrightarrow g_3 < I_b < g_8 \equiv g_4 + \frac{c_1(\mu + d - \beta S_b)}{\beta c_3}. \tag{4.5}$$

The proof is lengthy, but trivial.

In (4.5), $g_3 < g_2 - \frac{c_1 c_2}{\beta c_3} < g_8 < g_4 < g_1$ since $h_1 < S_b < h_2$ yields $-\frac{c_1 c_2}{\beta c_3} < \frac{c_1(\mu + d - \beta S_b)}{\beta c_3} < 0$.

Corollary 4.2 *The pseudoequilibria E_{S1} and E_{S3} are mutually exclusive.*

We note that $h_1 < S_b < h_2$ implies that $g_2 < g_4 < g_1$; this last inequality will play a crucial role in the cases below.

4.2 Sliding mode on M_2 and its dynamics

By Definition 3.3, the sliding domain $\Omega_2 \subset M_2$ for $I < g_4$ is given by (3.8), and there is no sliding domain for $I > g_4$. As we have seen, we get $g_2 < g_4 < g_1$ from $h_1 < S_b < h_2$. Moreover, $h_1 < S_b < h_2$ yields

$$g_3 < \frac{\Lambda\beta - (\mu + c_1)(\mu + d + c_2)}{\beta(\mu + d + c_2)} < g_5 < \frac{\Lambda\beta - (\mu + d)(\mu + c_1)}{\beta(\mu + d)} < g_1.$$

The sliding mode on Ω_2 is governed by Eq. (3.10) and the sliding equilibrium $E_{S2} = (S_b, g_6)$, if present in the system, is unstable on $\Omega_2 \subset M_2$ as proven in Theorem 3.4. Since $g_6 = g_4 - \frac{c_1}{\beta} + \frac{c_1(\mu + d + c_3 - \beta S_b)}{\beta(c_3 - c_2)} > g_4$ whenever $h_1 < S_b < h_2$, then $E_{S2} \notin \Omega_2 \subset M_2$.

4.3 Stability of the endemic states

For a fixed threshold level S_b such that $h_1 < S_b < h_2$, E_{21} is a virtual equilibrium and so it is not present in system (2.1). However, E_{11} and E_{31} are real equilibria if $E_{11} \in G_1$ and $E_{31} \in G_3$, respectively. In the following subsections, we are going to study the stability of the endemic states that we will illustrate with several numerical simulations. The associated parameters involved in the numerical simulations are defined in Table 1.

4.3.1 Case 4: $I_b < g_3 < g_2 < g_1$

Under these conditions, E_{11} and E_{21} are virtual equilibria, whereas E_{31} is a real equilibrium. It follows from Proposition 4.1 that E_{S1} and E_{S3} are not pseudoequilibria; namely, $E_{S1} \notin \Omega_4$ and $E_{S3} \notin \Omega_3$.

Proceeding as we did for Theorem 3.5, we get the following result.

Theorem 4.3 *E_{31} is globally asymptotically stable for $I_b < g_3 < g_2 < g_1$ and $R_1 > 1$.*

Theorem 4.3 is illustrated in Fig. 5 with $S_b = 2$ and $I_b = 1$. All solutions with any initial conditions in $\mathbb{R}^2_+$ converge to E_{31} as t increases.

4.3.2 Case 5: $g_3 < I_b < g_2 < g_1$

In the present case, E_{11}, E_{21} and E_{31} are virtual equilibria and so not present in the system (2.1). This case must be divided in two subcases: $g_8 > g_2$ and $g_8 < g_2$.

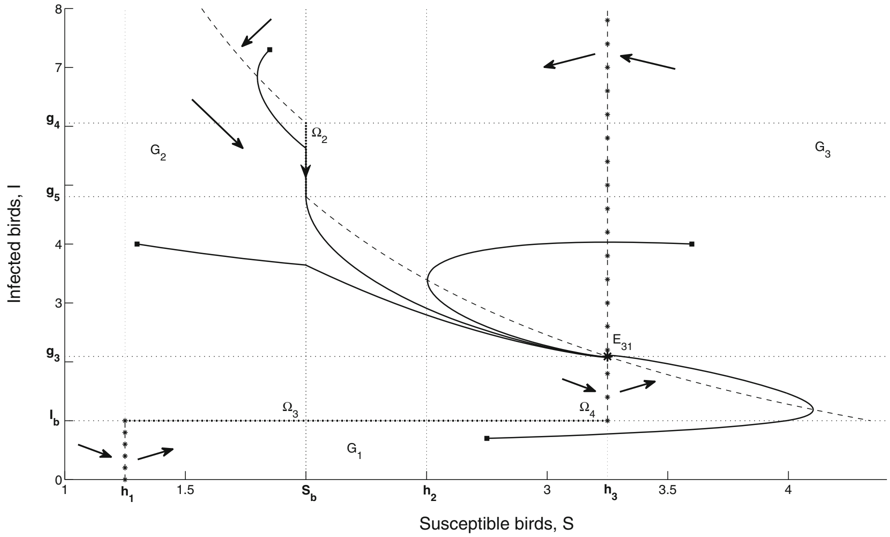

Fig. 5 E_{31} is globally asymptotically stable for $h_1 < S_b < h_2$, $I_b < g_3 < g_2 < g_1$ and $R_1 > 1$

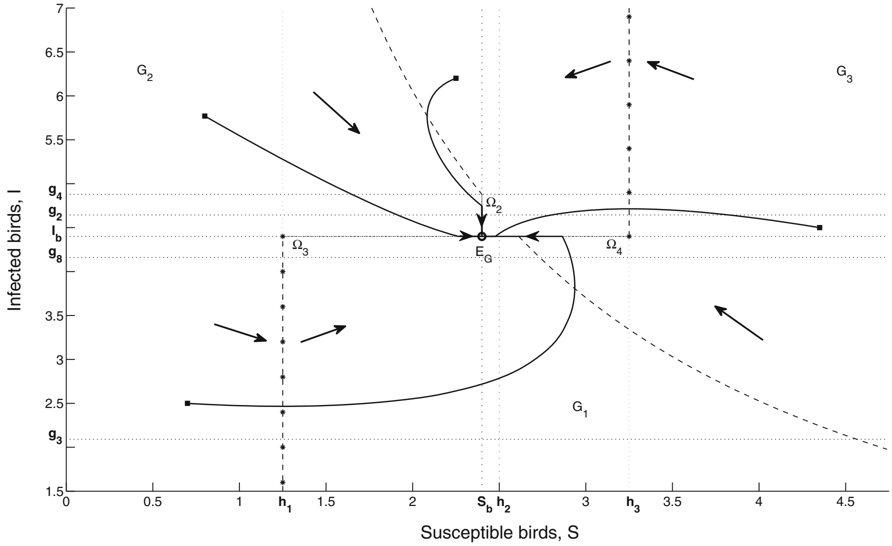

Fig. 6 E_G is a global pseudo-attractor whenever $h_1 < S_b < h_2$, $g_3 < g_8 < I_b < g_2 < g_1$ and $R_1 > 1$

First, we note that E_{S3} is not a pseudoequilibrium in the present case. Moreover, using a technique similar to the one used in the proof of the non-existence of limit cycles in Theorem 3.2, the reader can prove the following theorem.

Theorem 4.4 *Since $g_3 < I_b < g_8$, then $E_{S1} \in \Omega_4 \subset M_1$ is globally asymptotically stable if $R_1 > 1$.*

If $g_3 < I_b < g_2 < g_8 < g_1$, the point $E_{S1} \in \Omega_4 \subset M_1$ is a globally asymptotically stable pseudoequilibrium. The phase space in this case is similar to the phase portrait represented in Fig. 3 and will not be given.

If $g_3 < I_b < g_8 < g_2$, then we have the same dynamic as above. However, if $g_3 < g_8 < I_b < g_2$, no equilibrium exists in the system. However, all orbits will converge in a finite time to $E_G = (S_b, I_b)$; we call such an attracting point a pseudo-attractor. The phase portrait in this case is represented in Fig. 6 with $S_b = 2.4$ and $I_b = 4.4$.

4.3.3 Case 6: $g_3 < g_2 < I_b < g_1$

We have that E_{11}, E_{21} and E_{31} are virtual equilibria; so, they are not present in (2.1). As in Case 5, we have to consider $g_8 < g_2$ and $g_8 > g_2$.

Recall that $g_2 < g_4 < g_1$ in Case B. If $g_4 < I_b < g_1$, independently of $g_8 < g_2$ or $g_8 > g_2$, it follows from (4.4) that E_{S3} is a pseudoequilibrium. Again, using an approach similar to the one used in the proof of the non-existence of limit cycles in Theorem 3.2, we get the following theorem.

Theorem 4.5 *If $g_4 < I_b < g_1$, then $E_{S3} \in \Omega_3 \subset M_1$ is globally asymptotically stable if $R_1 > 1$.*

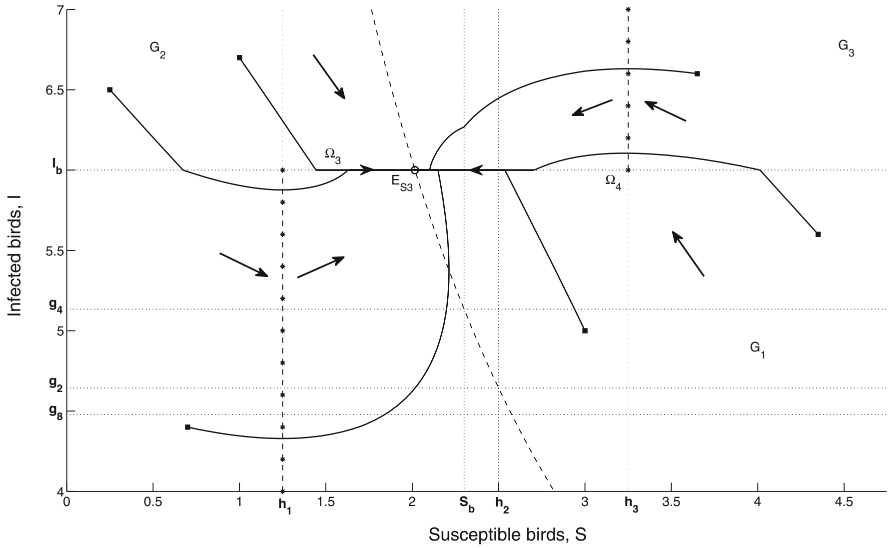

Fig. 7 $E_{S3} \in \Omega_3 \subset M_1$ is a globally asymptotically stable pseudoequilibrium if $h_1 < S_b < h_2$, $g_3 < g_8 < g_2 < g_4 < I_b < g_1$ and $R_1 > 1$

If $g_8 < g_2 < g_4 < I_b < g_1$ or $g_2 < g_8 < g_4 < I_b < g_1$, we get the same phase space. So for this case, we only depict the numerical result of $g_3 < g_8 < g_2 < g_4 < I_b < g_1$ with $S_b = 2.3$ and $I_b = 6$, which is as shown in Fig. 7.

If $g_2 < g_8 < I_b < g_4 < g_1$ or $g_8 < g_2 < I_b < g_4 < g_1$, then no equilibrium can be found in this system and E_G becomes again a global pseudo-attractor. The phase portrait for the case $g_2 < g_8 < I_b < g_4 < g_1$ is given in Fig. 8, where $S_b = 2.2$ and $I_b = 5$.

Finally, if $g_2 < I_b < g_8$, then we may use Theorem 4.4 to conclude that E_{S1} is a globally asymptotically stable pseudoequilibrium. The point E_{S3} is not a pseudoequilibrium according to (4.4). The phase portrait of this case is similar to the phase portrait in Fig. 3.

4.3.4 Case 7: $g_3 < g_2 < g_1 < I_b$

In this case, E_{21} and E_{31} are not equilibria for (2.1), but E_{11} is an equilibrium. Moreover, E_{S3} and E_{S1} are not pseudoequilibria as the requirements of (4.2) and (4.3) are not met, according to Proposition 4.1.

Theorem 4.6 *The equilibrium E_{11} is globally asymptotically stable if $I_b > g_1$ and $R_1 > 1$.*

The proof of this theorem is identical to the proof of Theorem 3.8 since E_{11} is asymptotically stable in G_1 by Theorem 2.4. It is globally asymptotically stable because there are no periodic orbits in G_1 and, eventually, all orbits enter the region G_1 and do not leave it. The phase portrait for this case is similar to Fig. 4.

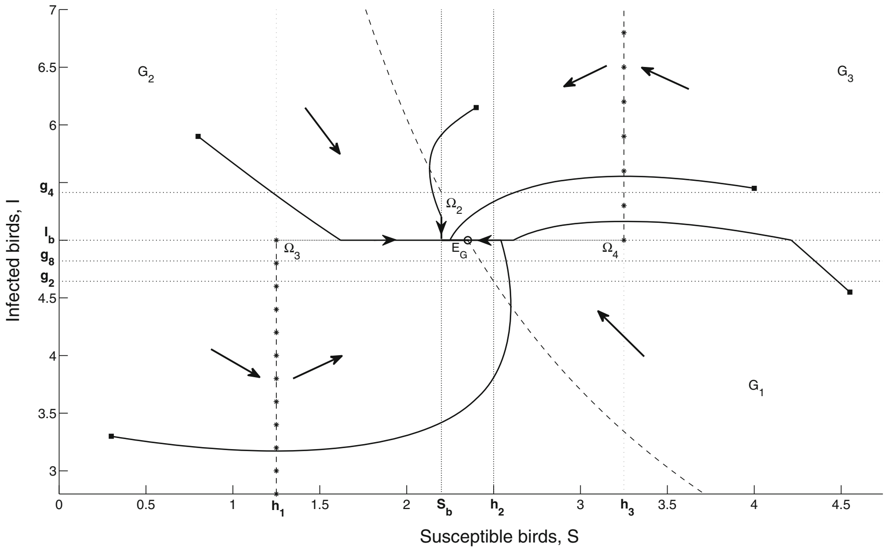

Fig. 8 E_G is a global attractor if $h_1 < S_b < h_2$ and $g_3 < g_2 < g_8 < I_b < g_4 < g_1$

5 Case C: $h_2 < S_b < h_3$

5.1 Sliding mode on M_1 and its dynamics

The sliding domains on M_1 are

$$\Omega_5 = \{(S, I) \in M_1; h_1 < S < h_2\} \quad \text{and} \quad \Omega_6 = \{(S, I) \in M_1; S_b < S < h_3\}.$$

The dynamics on Ω_5 are governed by (4.1), whereas the dynamics on Ω_6 are governed by (3.2).

$E_{S3} = (h_5, I_b)$ and $E_{S1} = (h_4, I_b)$ are the sliding equilibria on Ω_5 and Ω_6, respectively. The following proposition gives the conditions for E_{S3} and E_{S1} to be pseudoequilibria.

Proposition 5.1 *Let* $g_7 = g_4 - \frac{c_1[\beta S_b - (\mu+d)]}{\beta c_3}$. *Since* $h_2 < S_b < h_3$, *we have* $g_3 < g_7 < g_4 < g_2$. *Moreover,*

$$S_b < h_4 < h_3 \Leftrightarrow g_3 < I_b < g_7 \tag{5.1}$$

and

$$h_1 < h_5 < h_2 \Leftrightarrow g_2 < I_b < g_1. \tag{5.2}$$

Thus E_{S1} is a pseudoequilibrium if $g_3 < I_b < g_7$ and E_{S3} is a pseudoequilibrium if $g_2 < I_b < g_1$.

5.2 Sliding mode on M_2 and its dynamics

Everything from Sect. 3.2 is still valid. In particular, the sliding region $\Omega_2 \subset M_2$ is defined in (3.8). There is a pseudoequilibrium $E_{S2} = (S_b, g_6)$ only if (3.11) is satisfied. It is always unstable.

We note that $h_2 < S_b < h_3$ yields $g_3 < g_5 < g_4 < g_2$. Moreover, since $S_b < h_3 = \frac{\mu+d+c_3}{\beta}$, we get

$$g_6 = \frac{c_1(\mu + d + c_3 - \beta S_b)}{\beta(c_3 - c_2)} + \frac{\Lambda - (\mu + c_1)S_b}{\beta S_b} > \frac{\Lambda - (\mu + c_1)S_b}{\beta S_b} = g_5,$$

and since $S_b > h_2 = \frac{\mu+d+c_2}{\beta}$, we get

$$g_6 = \frac{c_1(\mu + d + c_3 - \beta S_b)}{\beta(c_3 - c_2)} + \frac{\Lambda - (\mu + c_1)S_b}{\beta S_b} = g_4 + \frac{c_1(\mu+d + c_2 - \beta S_b)}{\beta(c_3 - c_2)} < g_4.$$

The condition (3.11) is therefore always satisfied and the pseudoequilibrium E_{S2} is always present if $I_b < g_6$.

5.3 Stability of the endemic states

A similar analysis as exhibited in Sects. 3.3 and 4.3 is applied here. For Case C, we pick $S_b = 3$ to execute several numerical simulations in order to demonstrate the theoretical results.

5.3.1 Case 8: $I_b < g_3 < g_2 < g_1$

In the present case, E_{21} and E_{31} are real equilibria, whereas E_{11} is a virtual equilibrium. Furthermore, there is no pseudoequilibrium other than E_{S2} whenever $I_b < g_3 < g_2 < g_1$. In the following theorem, it is proven that E_{21} and E_{31} are locally asymptotically stable.

Theorem 5.2 *If $h_2 < S_b < h_3$, then E_{21} is locally asymptotically stable for $I_b < g_2$ and E_{31} is locally asymptotically stable for $I_b < g_3$.*

Proof The linearization $J_2(E_{21})$ of (2.1) at E_{21} has the eigenvalues

$$\lambda_{\pm} = \frac{1}{2}\left\{-\frac{\Lambda\beta}{\mu + d + c_2} \pm \sqrt{\triangle_2}\right\}$$

where

$$\triangle_2 = \left(\frac{\Lambda\beta}{\mu + d + c_2}\right)^2 - 4\big[\Lambda\beta - \mu(\mu + d + c_2)\big].$$

Since $I_b < g_2$, we have $\Lambda\beta - \mu(\mu + d + c_2) > \beta I_b(\mu + d + c_2) > 0$, where all associated parameters are positive. Thus $\triangle_2 < \left(\frac{\Lambda\beta}{\mu+d+c_2}\right)^2$. Hence the real part of $\lambda_\pm$ is always negative. We can have $\triangle_2 \geq 0$ or $\triangle_2 < 0$; thus E_{21} is either a stable node in the first case or a stable spiral in the latter case.

A similar argument shows that E_{31} is also locally asymptotically stable if $I_b < g_3 < g_2 < g_1$. □

Since there are no periodic orbits in $\mathbb{R}^2_+$, almost all solutions of (2.1) in $\mathbb{R}^2_+$ will converge to either E_{21} or E_{31} as $t \to \infty$. The exceptions are the two orbits associated to the stable manifold of the equilibrium E_{S2}; together, they form the separatrix between the ω-limit sets of E_{21} and E_{31}.

Figure 9 displays the phase portrait for Case 8 with $I_b = 1$.

5.3.2 Case 9: $g_3 < I_b < g_2 < g_1$

In this case, E_{21} is a real equilibrium, but E_{11} and E_{31} are virtual equilibria. We also have that E_{S2} is an unstable pseudoequilibrium as long as $I_b < g_6$.

A simple computation gives

$$h_2 < S_b < h_3 \Leftrightarrow g_5 < g_7 < g_4 - \frac{c_1 c_2}{\beta c_3}.$$

Proposition 5.3 *Since $c_3 > c_2 > 0$ and $h_2 < S_b < h_3$, then*

$$g_6 = g_7 + \frac{c_1 c_2 (\mu + d + c_3 - \beta S_b)}{\beta c_3 (c_3 - c_2)} > g_7.$$

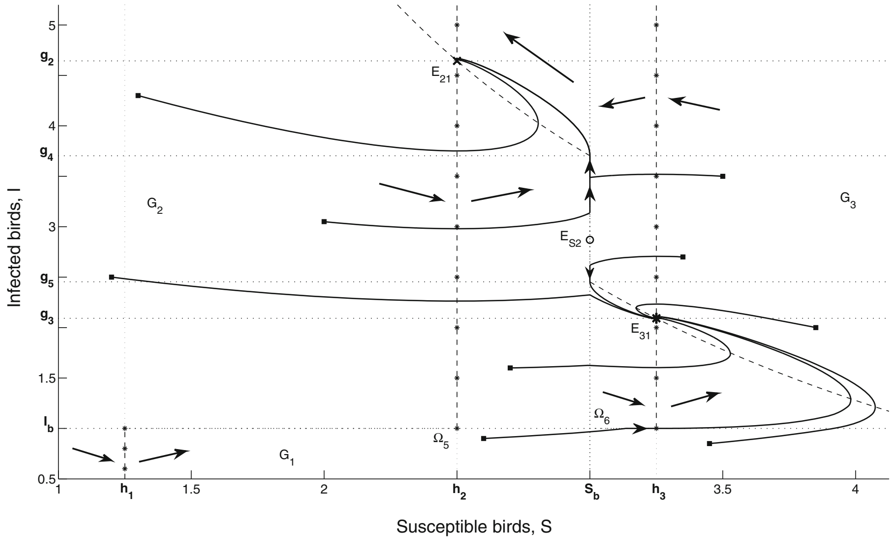

Fig. 9 E_{21} and E_{31} are locally asymptotically stable if $h_2 < S_b < h_3$, $I_b < g_3 < g_2 < g_1$ and $R_1 > 1$

Hence $g_3 < g_5 < g_7 < g_6 < g_4 < g_2 < g_1$.

This is a consequence of the fact that $h_2 < S_b < h_3$ implies $0 < \mu + d + c_3 - \beta S_b < c_3 - c_2$.

If $g_3 < I_b < g_7$, we have one equilibrium, E_{21}, and two pseudoequilibria, E_{S1} and E_{S2}. We have seen in Theorem 5.2 that E_{21} is locally asymptotically stable, and in Theorem 3.4 that E_{S2} is always unstable. The following theorem addresses the stability of E_{S1}.

Theorem 5.4 *$E_{S1} \in \Omega_6 \subset M_1$ is locally asymptotically stable if $g_3 < I_b < g_7$.*

Proof $E_{S1} \in \Omega_6 \subset M_1$ is locally asymptotically stable since

$$\frac{\partial}{\partial S}\left(\frac{-\beta c_1 S^2 + (c_1(\mu + d) - c_3(\beta I_b + \mu))S + \Lambda c_3}{c_3}\right)\Bigg|_{h_4}$$
$$= \frac{-2\beta c_1 S + c_1(\mu + d) - c_3(\mu + \beta I_b)}{c_3}\Bigg|_{h_4} = \frac{-\sqrt{B^2 - 4AC}}{c_3} < 0,$$

where $c_3, \sqrt{B^2 - 4AC} > 0$. □

Hence the orbits in $\mathbb{R}^2_+$ of the system (2.1) will either converge to E_{S1} or E_{21} as t increases except for the two orbits associated to the stable manifold of the unstable pseudoequilibrium E_{S2}. The phase portrait for this case can be found in Fig. 10 with $I_b = 2.3$.

If $g_7 < I_b < g_6$, the system (2.1) has a pseudo-attractor E_G, a locally asymptotically stable equilibrium E_{21} and an unstable pseudoequilibrium E_{S2}. All trajectories

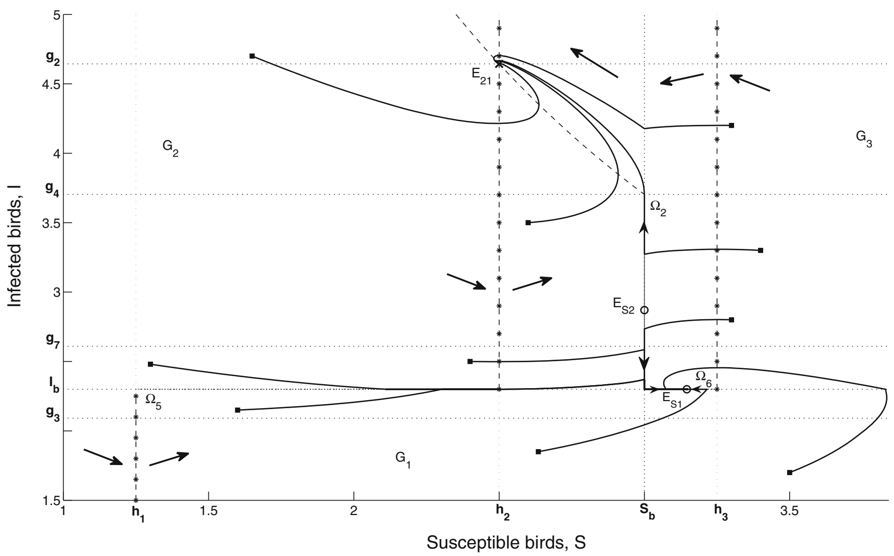

Fig. 10 E_{21} and $E_{S1} \in \Omega_6 \subset M_1$ are locally asymptotically stable if $h_2 < S_b < h_3$ and $g_3 < I_b < g_7 < g_6 < g_4 < g_2 < g_1$

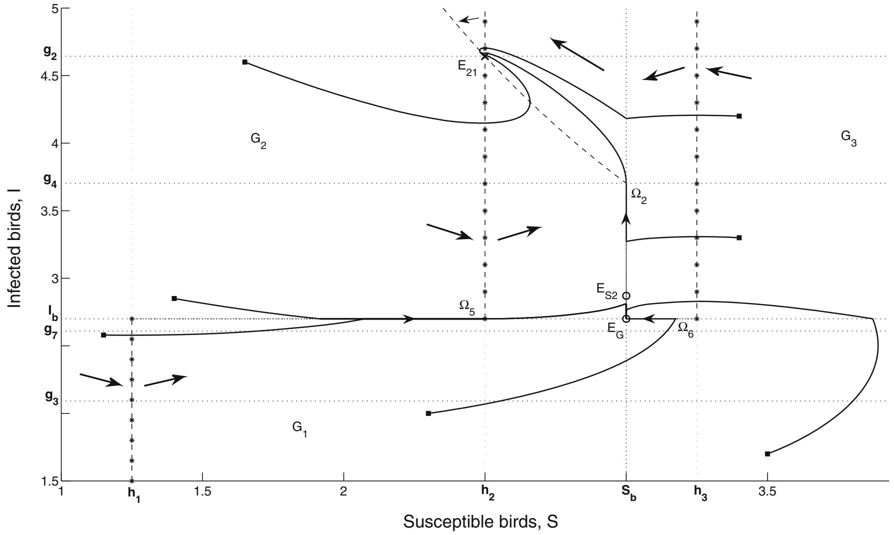

Fig. 11 E_{21} is locally asymptotically stable and E_G is a pseudo-attractor if $h_2 < S_b < h_3$ and $g_3 < g_7 < I_b < g_6 < g_4 < g_2 < g_1$

with arbitrary initial points in $\mathbb{R}^2_+$ will either converge to E_{21} or E_G as t increases. The two orbits associated to the stable manifold of the unstable pseudoequilibrium E_{S2} form a separatrix between the ω-limit sets of E_{21} and E_G. The phase portrait of this system is given in Fig. 11, where $I_b = 2.7$.

If $g_6 < I_b < g_2$, we have only the equilibrium E_{21}. Therefore E_{21} is globally asymptotically stable. The phase portrait of the system for $g_6 < I_b < g_4 < g_2$ is given in Fig. 12, where $I_b = 3.2$. The phase portrait for the case $g_6 < g_4 < I_b < g_2$ is qualitatively similar to the one given in Fig. 12 and is not given here.

5.3.3 Case 10: $g_3 < g_2 < I_b < g_1$

E_{11}, E_{21} and E_{31} are all virtual equilibria. Moreover, from (4.5), we find that E_{S1} is not a pseudoequilibrium because $I_b > g_2 > g_7$ and the sliding domain on M_2 (i.e., Ω_2) does not exist as $I_b > g_2 > g_4$. The system (2.1) has only the pseudoequilibrium E_{S3} since (5.2) is fulfilled.

The following theorem proves that $E_{S3} \in \Omega_5 \subset M_1$ is globally asymptotically stable.

Theorem 5.5 *$E_{S3} \in \Omega_5 \subset M_1$ is globally asymptotically stable if $h_2 < S_b < h_3$, $g_3 < g_2 < I_b < g_1$ and $R_1 > 1$.*

The proof of Theorem 5.5 is similar to the proof of Theorem 3.2.

Furthermore, the phase portrait of Case 10 is described in Fig. 13, where $I_b = 7$.

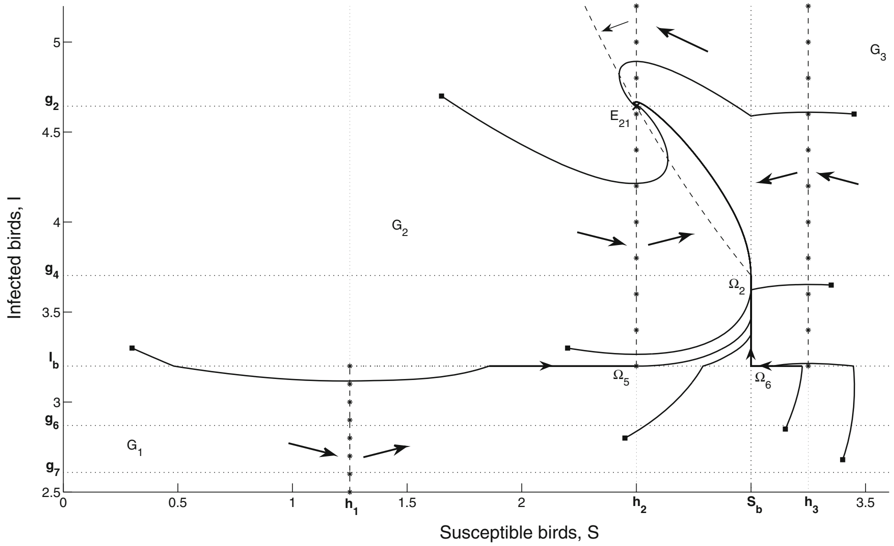

Fig. 12 E_{21} is globally asymptotically stable if $h_2 < S_b < h_3$ and $g_3 < g_7 < g_6 < I_b < g_4 < g_2 < g_1$

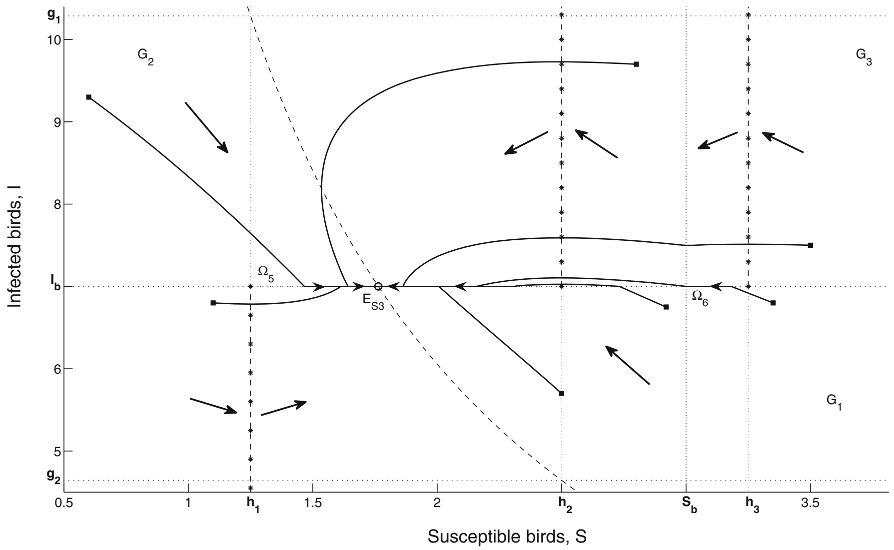

Fig. 13 $E_{S3} \in \Omega_5 \subset M_1$ is globally asymptotically stable if $h_2 < S_b < h_3$, $g_3 < g_2 < I_b < g_1$ and $R_1 > 1$

5.3.4 Case 11: $g_3 < g_2 < g_1 < I_b$

E_{21} and E_{31} are virtual equilibria, and E_{11} is a real equilibrium. It also follows from Sects. 5.1 and 5.2 that there are no pseudoequilibria. We show below that E_{11} is globally asymptotically stable. Case 11 is similar as Case 7.

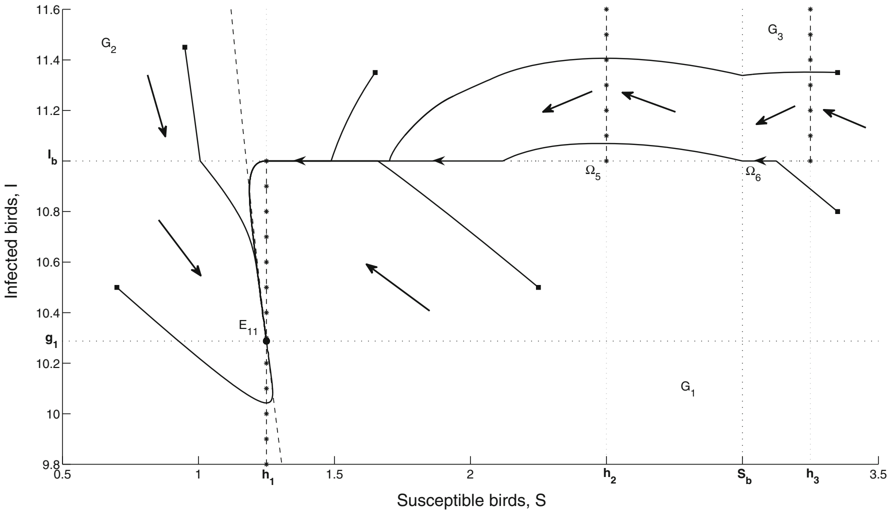

Fig. 14 E_{11} is globally asymptotically stable if $h_2 < S_b < h_3$, $g_3 < g_2 < g_1 < I_b$ and $R_1 > 1$

Theorem 5.6 *E_{11} is globally asymptotically stable if $h_2 < S_b < h_3$, $g_3 < g_2 < g_1 < I_b$ and $R_1 > 1$.*

The proof of this theorem is similar to the proof of Theorem 4.6, and so it is omitted. The phase portrait for this case is given in Fig. 14.

6 Case D: $S_b > h_3$

6.1 Sliding mode on M_1 and its dynamics

There exists a sliding domain $\Omega_5 = \{(S, I) \in M_1 : h_1 < S < h_2\}$ on M_1 and its dynamics are governed by (4.1). The sliding equilibrium $E_{S3} = (h_5, I_b) \in \Omega_5 \subset M_1$ is a pseudoequilibrium if (5.2) is satisfied.

6.2 Sliding mode on M_2 and its dynamics

We have that $\langle n_2, f_2\rangle > 0$ and $\langle n_2, f_3\rangle < 0$ for $g_5 < I < g_4$ as in Sect. 3.2. Furthermore, $S_b > h_3$ implies that

$$g_5 = \frac{\Lambda}{\beta S_b} - \frac{\mu + c_1}{\beta} < \frac{\Lambda}{\mu + d + c_3} - \frac{\mu + c_1}{\beta} = g_3$$

and similarly $g_4 < g_2$. Recall that

$$\Omega_2 = \{(S, I) \in M_2 : \max\{g_5, I_b\} < I < g_4\}$$

for $I_b < g_4$, while Ω_2 does not exist if $I_b \geq g_4$. The dynamics on Ω_2 are governed by (3.10). Furthermore, $h_3 < S_b$ implies that

$$g_6 = \frac{c_1(\mu + d + c_3 - \beta S_b)}{\beta(c_3 - c_2)} + \frac{\Lambda - (\mu + c_1)S_b}{\beta S_b} < \frac{\Lambda - (\mu + c_1)S_b}{\beta S_b} = g_5.$$

Thus $E_{S2} = (S_b, g_6)$ is never a pseudoequilibrium for $h_3 < S_b$.

6.3 Stability of the endemic states

The same approach as shown in Sects. 3.3, 4.3 and 5.3 is implemented in this section. E_{31} is always a virtual equilibrium because of $S_b > h_3$. Several numerical simulations are performed in this section by choosing $S_b = 4$.

6.3.1 Case 12: $I_b < g_3 < g_2 < g_1$ or $g_3 < I_b < g_2 < g_1$

There is only one equilibrium at E_{21}. The points E_{11} and E_{31} are virtual equilibria, and E_{S2} and E_{S3} are not pseudoequilibria. A simple analysis with the nullclines as we have done for the proof of Theorem 3.8 gives the following result.

Theorem 6.1 *E_{21} is globally asymptotically stable if $I_b < g_3 < g_2 < g_1$ or $g_3 < I_b < g_2 < g_1$, $S_b > h_3$ and $R_1 > 1$.*

Figure 15 depicts the numerical result of $I_b < g_3 < g_2 < g_1$. We choose $I_b = 1$ in Fig. 15. The numerical result of $g_3 < I_b < g_2 < g_1$ is omitted here since it is similar to Fig. 15.

6.3.2 Case 13: $g_3 < g_2 < I_b < g_1$

In this case, E_{11}, E_{21} and E_{31} are virtual equilibria. As we said before, E_{S2} is not a pseudoequilibrium. There is only one pseudoequilibrium E_{S3} in system (2.1). The phase portrait for this case is given in Fig. 16, where $I_b = 6$.

6.3.3 Case 14: $g_3 < g_2 < g_1 < I_b$

The equilibrium E_{11} is globally asymptotically stable whenever $g_3 < g_2 < g_1 < I_b$. The points E_{21} and E_{31} are virtual equilibrium, and E_{S2} and E_{S3} are not pseudoequilibria.

Theorem 6.2 *E_{11} is globally asymptotically stable if $S_b > h_3$, $g_3 < g_2 < g_1 < I_b$ and $R_1 > 1$.*

The numerical result of this case is relatively similar to the phase portrait given in Fig. 4.

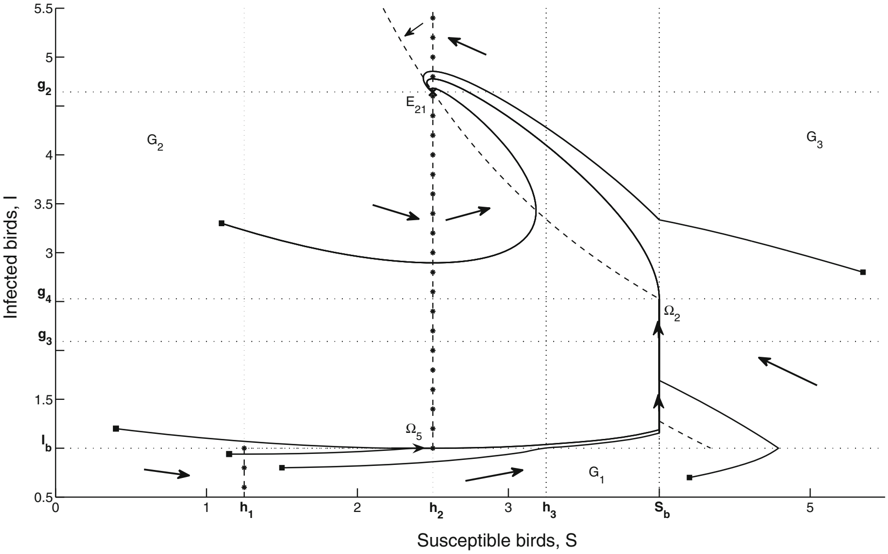

Fig. 15 E_{21} is globally asymptotically stable if $S_b > h_3$, $I_b < g_3 < g_2 < g_1$ and $R_1 > 1$

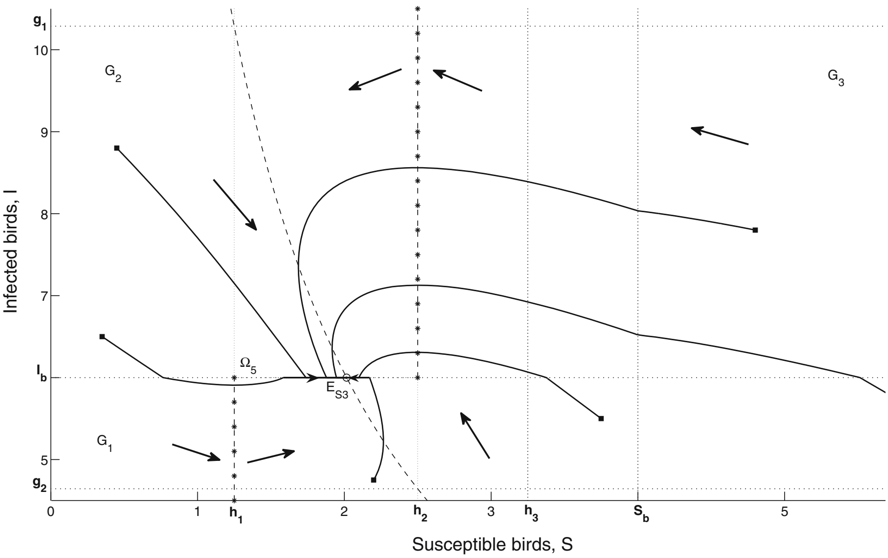

Fig. 16 $E_{S3} \in \Omega_5 \subset M_1$ is globally asymptotically stable if $S_b > h_3$, $g_3 < g_2 < I_b < g_1$ and $R_1 > 1$

7 Conclusion and discussion

The model we considered here used nonlinear ordinary differential equations with discontinuous right-hand sides, extending our previous work (Chong and Smith? 2015) by taking into account culling susceptible birds, instead of only infected birds. Since culling birds is one of the most effective strategies to control the transmission of bird

Table 2 Conclusions for Sects. 3–6

<table>
<tr><td></td><td>$S_b < h_1$</td><td>$h_1 < S_b < h_2$</td><td>$h_2 < S_b < h_3$</td><td>$S_b > h_3$</td></tr>
<tr><td>$I_b < g_3$</td><td>II</td><td>II</td><td>IV</td><td>II</td></tr>
<tr><td rowspan="3">$g_3 < I_b < g_2$</td><td rowspan="3">I</td><td>$I_b < g_8$: I</td><td>$I_b < g_7 < g_6 < g_4$: III</td><td rowspan="3">II</td></tr>
<tr><td rowspan="2">$g_8 < I_b$: I</td><td>$g_7 < I_b < g_6 < g_4$: III</td></tr>
<tr><td>$g_6 < I_b$: II</td></tr>
<tr><td rowspan="3">$g_2 < I_b < g_1$</td><td rowspan="3">I</td><td>$I_b < g_8 < g_4$: I</td><td rowspan="3">I</td><td rowspan="3">I</td></tr>
<tr><td>$g_8 < I_b < g_4$: I</td></tr>
<tr><td>$g_8 < g_4 < I_b$: I</td></tr>
<tr><td>$g_1 < I_b$</td><td>I</td><td>I</td><td>I</td><td>I</td></tr>
</table>

flu, it was also essential for us to look into other efficient culling strategies that not only control the disease, but reduce the socio-economic impact as well (FAO 2008; Centers for Disease Control and Prevention 2012; International Animal Health Organisation 2015; Gulbudak and Martcheva 2013; Menach et al. 2006). To achieve this objective, the numbers of susceptible and infected birds were employed as reference indices in our disease-management strategy in order to determine whether or not we need to call for culling birds as a control measure.

In this model, depopulation of birds was only carried out if the number of infected birds was greater than the threshold level I_b; no application of culling strategy was carried out whenever the number of infected birds was below the threshold level I_b. When the number of infected birds was above I_b, infected birds were culled with rates c_2 and c_3 if the numbers of susceptible birds were less than or greater than the threshold level S_b, respectively. Moreover, we culled susceptible birds with rate c_1 if the number of susceptible birds exceeded the threshold level S_b, in order to prevent a serious infection among the avian population.

The results from Sects. 3–6 are summarised in Table 2, with the following biological outcomes:

I. For these choices of infected and susceptible threshold levels I_b and S_b, there is no risk of an epidemic because the infected level will always eventually converge to a level below or equal to I_b, as we can see from Figs. 3, 4, 6, 7, 8, 12, 13, 14 and 16. In these cases, there is a globally asymptotically stable equilibrium, pseudoequilibrium or pseudo-attractor below or on $I = I_b$.

II. It is virtually impossible to avoid an epidemic if the infected threshold level I_b is sufficiently low. As can be seen in Figs. 2, 5 and 15, as soon as there are some infected birds, the number will rise above I_b to reach the level of a globally asymptotically stable equilibrium.

III. If there are initially a small number of infected birds, this number may rise but will stay at a level inferior or equal to the infected threshold level I_b. However, if there are initially too many infected birds, the number of infected birds will balloon to a level higher than I_b. As can be seen in Figs. 10 and 11, for initial conditions with the number of infected birds I small enough, the orbits will converge to a pseudo-attractor or a locally stable pseudoequilibrium on $I = I_b$. However, for initial conditions with $I(0)$ large enough, the orbits will converge to the locally asymptotically stable equilibrium above $I = I_b$.

IV. This case is similar to Case II, in the sense that it is impossible to avoid an epidemic. However, the reason for this conclusion is slightly different. As seen in Fig. 9, there are two locally asymptotically stable equilibria. Since both are above the infected threshold level I_b, the number of infected birds will converge to one of these equilibria, depending on initial conditions, and an epidemic will ensue.

In Case I, there is no need to modify the culling policy. The number of infected birds will eventually be below the infected threshold level I_b. In Cases II and IV, the infected threshold level is not realistic for this bird population and must be modified.

In Case III, there may not be any need to modify the culling policy if the initial number of infected birds is kept low. However, there is a risk of epidemic if there is a large inflow of infected birds.

Our model has several limitations, which should be acknowledged. We assumed that the bird inflow in this model was a fixed constant, the culling rate c_3 was greater than the culling rate c_2 and infected birds were presumed not to move to other classes; i.e., the infected birds will only remain within the infected class. We also assumed mass action transmission, which carries with it the assumption of homogeneous contact.

In addition, a deterministic model like (2.1) is valid as long as we consider a large, well-mixed and homogeneous population in a limited area. This is the situation that we have in most large-scale industrial bird farms. If some of these conditions are not respected and the randomness in the evolution of a disease has to be considered, then a stochastic model will become more appropriate. This is, however, out of the scope of this paper. Stochastic effects are important for determining the viability of a population when the number of infected individuals is low or sparsely distributed; an epidemic that would be predicted to balloon may not if there were very few individuals. However, when dealing with large, dense populations, a threshold policy provides guidance for stemming a large-scale outbreak.

Our results have demonstrated that, by choosing appropriate threshold levels S_b and I_b, the avian influenza outbreak could either be prevented or at least stabilized at a desired level. However, we could suppress the infection of avian influenza by culling susceptible and/or infected birds whenever an avian influenza outbreak emerges. Hence, in order for us to combat or eradicate influenza in the avian population efficiently, a good threshold policy is required.

Acknowledgments The authors would like to thank the referees for all their valuable comments. NSC acknowledges support from the Ministry of Higher Education, Malaysia, and the School of Informatics and Applied Mathematics, Universiti Malaysia Terengganu. BD is supported by the University of Ottawa. RJS is supported by an NSERC Discovery Grant. For citation purposes, please note that the question mark in "Smith?" is part of his name.

References

Avian influenza—background (2006) Tech. rep., Food and Agriculture Organization. http://www.fao.org/avianflu/en/background.html

Chong NS, Smith? RJ (2015) Modelling avian influenza using filippov systems to determine culling of infected birds and quarantine. Nonlinear Anal Real World Appl 24:196–218

Dorigatti I, Mulatti P, Rosà R, Pugliese A, Busani L (2010) Modelling the spatial spread of H7N1 avian influenza virus among poultry farms in italy. Epidemics 2:39–35

Fact sheet—avian influenza (2012) Tech. rep., Canadian Food Inspection Agency. http://www.inspection.gc.ca/animals/terrestrial-animals/diseases/reportable/ai/fact-sheet/eng/1356193731667/1356193918453
Filippov AF (1988) Differential equations with discontinuous right-hand sides. Kluwer Academic Dordrecht, The Nertherlands
Food and Agriculture Organization of the United Nations (2011) Approaches to controlling, preventing and eliminating H5N1 highly pathogenic avian influenza in endemic countries. Tech. rep., Food and Agriculture Organization. http://www.fao.org/docrep/014/i2150e/i2150e.pdf
Food-producing animals: disease outbreaks (avian influenza h5n1) (2015) Tech. rep., International Animal Health Organisation—Europe. http://www.ifaheurope.org/food-producing-animals/disease-outbreaks/avianflu.html
Gulbudak H, Martcheva M (2013) Forward hysteresis and backward bifurcation caused by culing in an avian influenza model. Math Biosci 246:202–212
Gumel AB (2009) Global dynamics of a two-strain avian influenza model. Int J Comput Math 86:85–108
Human health issues related to avian influenza in canada (2006) Tech. rep., Public Health Agency of Canada. http://www.phac-aspc.gc.ca/publicat/daio-enia/2-eng.php#jmp-lan2
Iwami S, Takeuchi Y, Korobeinikov A, Liu X (2008) Prevention of avian influenza epidemic: what policy should we choose? J Theor Biol 252:732–741
Iwami S, Takeuchi Y, Liu X (2009) Avian flu pandemic: can we prevent it? J Theor Biol 257:181–190
Jacob JP, Butcher GD, Mather FB, Miles RD (2013) Avian influenza in poultry. University of Florida IFAS Extension ps38. http://edis.ifas.ufl.edu/ps032
Kimman T, Hoek M, de Jong MCM (2013) Assessing and controlling health risks from animal husbandry. NJAS Wagening J Life Sci 66:7–14
Le Menach A, Vergu E, Grais RF, Smith? DL, Flahault A (2006) Key strategies for reducing spread of avian influenza among commercial poultry holdings: lessons for transmission to humans. Proc R Soc B 273:2467–2475
Leine RI (2000) Bifurcations in discontinuous mechanical systems of Filippov-type. The Universiteitsdrukkerij TU Eindhoven, The Netherlands
Li J, Blakeley D, Smith? RJ (2011) The failure of r_0. Comp Math Methods Med ID 527610
Martcheva M (2014) Avian flu: modeling and implications for control. J Bio Syst 22(1):151–175
Perez DR, Garcia-Sastre A (2013) H5N1, a wealth of knowledge to improve pandemic preparedness. Virus Res 178:1–2
Perko L (2001) Differential equations and dynamical systems, 3rd edn. Springer, New York
Seasonal influenza (flu) (2012) Tech. rep., Centers for Disease Control and Prevention. http://www.cdc.gov/flu/avianflu/avian-in-birds.html
Shim E, Galvani AP (2009) Evolutionary repercussions of avian culling on host resistance and influenza virulence. PLoS One 4(5):e5503
Tang S, Xiao Y, Wang N, Wu H (2012) Piecewise HIV virus dynamic model with CD4^{+} T cell count-guided therapy. Theor Biol 308:123–134
The global strategy for prevention and control of H5N1 highly pathogenic avian influenza (2008) Tech. rep., Food and Agriculture Organization. ftp://ftp.fao.org/docrep/fao/011/aj134e/aj134e00.pdf
Tuncer N, Martcheva M (2013) Modeling seasonality in avian influenza H5N1. J Bio Syst 22(4):1340004
van den Driessche P, Watmough J (2002) Reproduction numbers and sub-threshold endemic equilibria for compartmental models of disease transmission. Math Biosci 180:29–48
Wang A, Xiao Y (2014) A filippov system describing media effects on the spread of infectious diseases. Nonlinear Anal Hybrid Syst 11:84–97
Xiao Y, Xu X, Tang S (2012) Sliding mode control of outbreaks of emerging infectious diseases. Bull Math Biol 74:2403–2422
Xiao Y, Zhao T, Tang S (2013) Dynamics of an infectious diseases with media/psychology induced non-smooth incidence. Math Biosci Eng 10(2):445–461
Zhao T, Xiao Y, Smith? RJ (2013) Non-smooth plant disease models with economic thresholds. Math Biosci 241:34–48